

The decoupled nature of basal metabolic rate and body temperature in endotherm evolution

Jorge Avaria-Llautureo^{1,2*}, Cristián E. Hernández³, Enrique Rodríguez-Serrano⁴ & Chris Venditti^{1*}

The origins of endothermy in birds and mammals are important events in vertebrate evolution. Endotherms can maintain their body temperature (T_b) over a wide range of ambient temperatures primarily using the heat that is generated continuously by their high basal metabolic rate (BMR)¹. There is also an important positive feedback loop as T_b influences BMR^{1–3}. Owing to this interplay between BMRs and T_b , many ecologists and evolutionary physiologists posit that the evolution of BMR and T_b must have been coupled during the radiation of endotherms^{3–5}, changing with similar trends^{6–8}. However, colder historical environments might have imposed strong selective pressures on BMR to compensate for increased rates of heat loss and to keep T_b constant^{9–12}. Thus, adaptation to cold ambient temperatures through increases in BMR could have decoupled BMR from T_b and caused different evolutionary routes to the modern diversity in these traits. Here we show that BMR and T_b were decoupled in approximately 90% of mammalian phylogenetic branches and 36% of avian phylogenetic branches. Mammalian BMRs evolved with rapid bursts but without a long-term directional trend, whereas T_b evolved mostly at a constant rate and towards colder bodies from a warmer-bodied common ancestor. Avian BMRs evolved predominantly at a constant rate and without a long-term directional trend, whereas T_b evolved with much greater rate heterogeneity and with adaptive evolution towards colder bodies. Furthermore, rapid shifts that lead to both increases and decreases in BMRs were linked to abrupt changes towards colder ambient temperatures—although only in mammals. Our results suggest that natural selection effectively exploited the diversity in mammalian BMRs under diverse, often-adverse historical thermal environments.

Phylogenetic statistical methods^{13,14} provide us with the opportunity to formally test whether BMR has been linked to T_b or ambient temperature (T_a) throughout the evolution of birds and mammals. By accommodating for and identifying heterogeneity in the rate of phenotypic evolution, these methods can detect and reconstruct accurate historical evolutionary processes¹⁵. Evaluation of the evolutionary coupling between BMR and T_b has direct consequences for several longstanding ecological and evolutionary theories^{2–8} (including the metabolic theory of ecology) that assume coupling between BMR and T_b .

We first quantified and compared rates of evolution for BMR and T_b along each branch of the time-calibrated phylogenetic trees of birds and mammals (hereafter, branch-wise rates (r); Methods). r is a rate scalar by which the background rate of evolution (σ^2_b) is multiplied to increase or decrease the pace of evolution; it measures how fast a trait evolved along an individual phylogenetic branch (Methods). If BMR and T_b were coupled during the evolution of endotherms, the amount of change along phylogenetic branches for both traits should be positively associated—in cases in which r_{BMR} is high, we expect it to be high for r_{T_b} (Fig. 1 b). We tested this prediction against alternative evolutionary scenarios. First, we cannot make any inferences about coupling or decoupling in cases in which there is no rate heterogeneity for both

BMR and T_b ($r = 1$ for all branches in the tree for both traits) (Fig. 1 a). Second, we infer decoupled evolution if both traits show rate heterogeneity, for which the magnitudes of r values are negatively correlated (that is, branches that evolve at a high rate for BMR but a low rate for T_b , and vice versa) (Fig. 1 c). We suggest this scenario indicates decoupled evolution because a negative correlation most probably indicates that one trait tends to be conserved while the other evolved rapidly. Third, we infer decoupled evolution if only one trait shows rate heterogeneity while the other evolved at a constant rate (Fig. 1 d, e) or if both traits show heterogeneity but the branch-wise rates are not associated (Fig. 1 f).

As BMR, body mass (M), T_b and T_a are—at least to some extent—correlated in extant birds and mammals, and such correlations may vary between orders¹⁶, we estimated the branch-wise rates for BMR and T_b while accounting for their covariates across extant species using the phylogenetic variable-rate regression model¹⁷ (Methods).

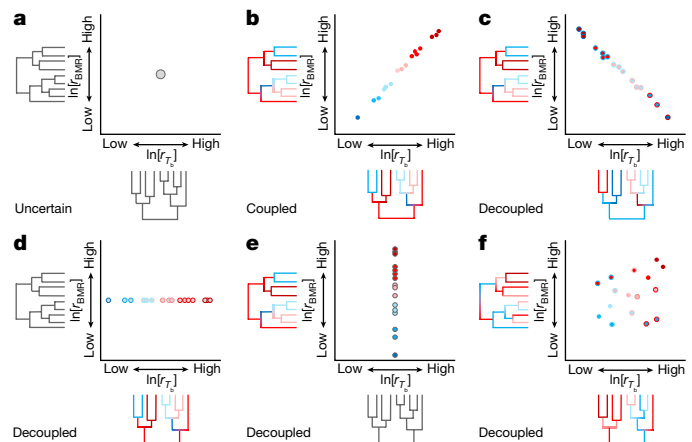


Fig. 1 | Possible evolutionary scenarios for BMR and T_b given their branch-wise rates in a bivariate space. **a**, Both traits evolve at a single constant rate across all branches of the tree ($r_{\text{BMR}} = 1$ and $r_{T_b} = 1$); in this case, we have no statistical power to evaluate an association between BMR and T_b . **b**, A positive correlation between r_{BMR} and r_{T_b} indicates that both traits are coupled—in cases in which BMR changed more, T_b also changed. **c**, A negative correlation between r_{BMR} and r_{T_b} implies that both traits are decoupled because when BMR changed more, T_b changed less. **d–f**, Correlations indicate that both traits are decoupled—when BMR evolved at a single constant rate, T_b evolved at a variable rate (**d**) or vice versa (**e**); or both traits evolved at variable rates ($r_{\text{BMR}} \neq 1$ and $r_{T_b} \neq 1$) but their magnitudes were not statistically correlated (**f**). Grey colour represents the constant background rate ($r = 1$). Red colours represent rates that are faster than the background rate ($r > 1$) and blue colours represent rates that are slower than the background rate ($r < 1$), which might be related to past events of positive¹⁷ and stabilizing selection²⁴, respectively. Point fill colours represent the magnitudes of r_{BMR} and point outline colours represent magnitudes of r_{T_b} .

¹School of Biological Sciences, University of Reading, Reading, UK. ²Centro de Investigación en Biodiversidad y Ambientes Sustentables (CIBAS), Facultad de Ciencias, Universidad Católica de la Santísima Concepción (UCSC), Concepción, Chile. ³Laboratorio de Ecología Evolutiva y Filoinformática, Departamento de Zoología, Facultad de Ciencias Naturales y Oceanográficas, Universidad de Concepción, Concepción, Chile. ⁴Laboratorio de Mastozoología, Departamento de Zoología, Facultad de Ciencias Naturales y Oceanográficas, Universidad de Concepción, Concepción, Chile. *e-mail: jorgeavariall@gmail.com; c.d.venditti@reading.ac.uk

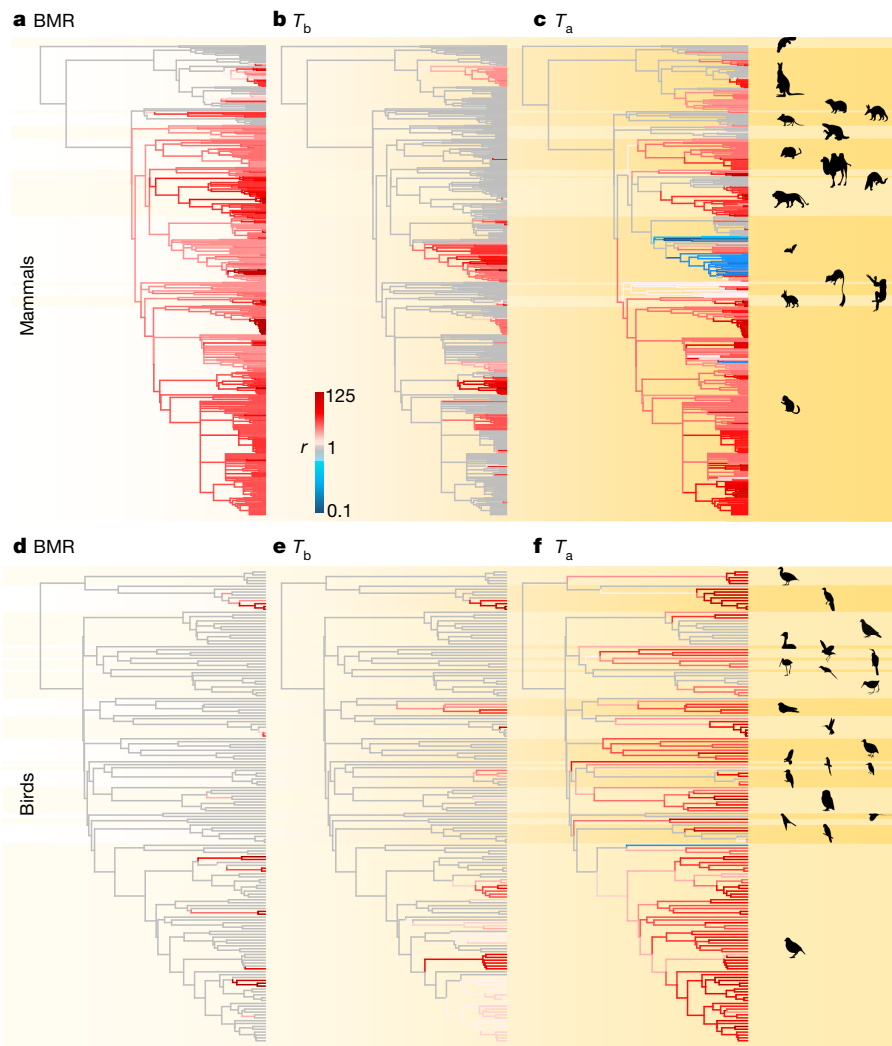


Fig. 2 | Branch-wise rates of BMR, T_b and T_a on the mammalian and avian phylogeny. **a–c**, Branch-wise rates for mammalian BMR (**a**), T_b (**b**) and T_a (**c**). **d–f**, Branch-wise rates for avian BMR (**d**), T_b (**e**) and T_a (**f**). The r values for each phylogenetic branch are shown in colours, and indicate whether the trait evolved at a constant background rate ($r = 1$, grey branches), at rates slower than the background rate ($r < 1$, blue-gradient branches) or at rates faster than the constant rate ($r > 1$, red-gradient branches). All silhouettes were obtained from <http://phylopic.org/>. Mammalian silhouettes were created by the following individuals (from top to bottom): Monotremata, S. Werning; Marsupialia, M. Callaghan; Hyracoidea, by S. Traver; Tubulidentata, P. Scott; Macroscelidea (uncredited); Pilosa, FunkMonk; Eulipotyphla, B. Barnes;

Artiodactyla, nicubunu; Pholidota, S. Traver; Carnivora (uncredited); Chiroptera, Y. Wong; Scandentia, T. M. Keeseey; Primates, T. M. Keeseey; Lagomorpha, A. Caravaggi; and Rodentia (uncredited). Avian silhouettes were created by the following individuals from top to bottom: Anseriformes, M. Martyniuk; Galliformes (uncredited); Columbiformes, F. Sayol; Podicipediformes, D. Backlund; Procellariiformes, M. Hannaford; Suliformes, F. Sayol; Pelecaniformes, S. Traver; Cuculiformes, F. Sayol; Gruiformes, F. Sayol; Caprimulgiformes, F. Sayol; Apodiformes, F. Sayol; Charadriiformes (uncredited); Accipitriformes, S. Traver; Bucerotiformes, S. Traver; Coraciiformes, F. Sayol; Piciformes, S. Traver; Strigiformes, F. Sayol, Coliiformes, E. J. Wetsy; Falconiformes, R. Groom; Psittaciformes, F. Sayol; and Passeriformes, P. Pattawaro.

This approach enables the simultaneous estimation of both an overall relationship between—for instance—BMR as a function of M and T_b across extant species, and any shifts in branch-wise rates that apply to the phylogenetically structured residual variance in the relationship. In both birds and mammals, the phylogenetic variable-rate regression model fits the data significantly better than the constant-rate regression models, which assume a single constant rate ($r = 1$) across all branches (Methods and Supplementary Tables 1–8). The best-fitting phylogenetic variable-rate regression model for mammalian BMR includes both M and T_b with a single slope for each trait that is estimated across all orders (Supplementary Tables 1, 2). For mammalian T_b , the best-fitting model includes M and BMR as covariates, also with a single slope across all orders (Supplementary Tables 3, 7). In birds, the best model for BMR includes only M , with a single slope for all orders (Supplementary Table 4). Finally, the best-fitting model for avian T_b includes M only in Columbiformes (Supplementary Table 6).

The branch-wise rates estimated for the best-fitting models show that mammalian BMR evolved at a constant rate ($r = 1$) in only 11.2% of branches and at faster rates ($r > 1$) in 88.8% of branches (Fig. 2a). Mammalian T_b evolved at a constant rate in 70.3% of branches and faster rates in 29.7% of branches (Fig. 2b). In birds, BMR evolved at a constant rate in 90.5% of branches and at faster rates in 9.5% of branches (Fig. 2d). Avian T_b evolved at a constant rate in 69% of branches and at faster rates in 31% (Fig. 2e). When the branch-wise rates for BMR and T_b were compared, we found that in mammals both traits evolved at a constant rate in 10.6% of branches (Fig. 3a, consistent with Fig. 1a). In 60.2% of branches, only one trait evolved at faster rates while the other trait diverged at a constant rate. This indicates that BMR and T_b evolved in a decoupled manner along these branches (Fig. 3a, consistent with Fig. 1d, e). We found that 29.2% of branches had an increased rate for both BMR and T_b . However, the magnitudes of the branch-wise rates were not significantly correlated (the percentage of the posterior distribution crossing zero as assessed by Bayesian Markov

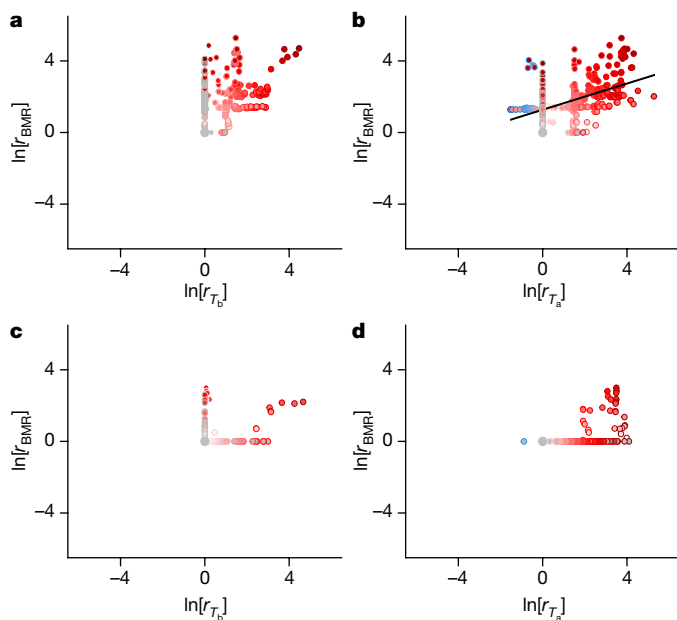


Fig. 3 | Branch-wise rates of BMR, T_b and T_a in bivariate space for mammals and birds. a, b, Bivariate space of mammals for r_{BMR} and r_{T_b} (a) or r_{T_a} (b). **c, d**, Bivariate space of birds for r_{BMR} and r_{T_b} (c) or r_{T_a} (d). **a**, In mammals, r_{BMR} was decoupled from r_{T_b} in 89.4% of branches because either only one trait showed rate heterogeneity while the other evolved a single constant rate (in 60.2% of branches; grey filled and red outlined dots, and grey outlined and red filled dots, consistent with Fig. 1d, e), or because both traits evolved at fast rates but the magnitudes of r_{BMR} and r_{T_b} were not correlated (in 29.2% of branches; red filled and outlined dots, consistent with Fig. 1f). In the remainder of the branches, 10.6%, (grey middle dot, consistent with Fig. 1a) there was no variation in either r_{BMR} or r_{T_b} . **b**, Bayesian generalized least squares analyses indicate that fast r_{BMR} and slow to fast r_{T_a} (red filled and blue and red outlined dots) were statistically correlated in 74.9% of mammalian branches ($P_{\text{MCMC}} = 0$; $n = 602$ branches; black line). In 18.2% of branches, the r_{BMR} was decoupled from r_{T_a} because only one trait shows rate heterogeneity (grey filled and red outlined dots and grey outlined and red filled dots). In the remainder of the branches, 6.9%, (grey middle dots), there was no variation in either r_{BMR} or r_{T_a} . **c**, In birds, r_{BMR} was decoupled from r_{T_b} in 36.2% of branches because either only 1 trait showed rate heterogeneity (in 32% of branches) or because the magnitude of fast rates in both traits were not correlated (in 4.2% of branches). There was no rate variation for either trait for the remaining 63.8% of branches. **d**, Avian r_{BMR} was decoupled from r_{T_a} in 77.9% of branches, because either only one trait showed rate heterogeneity (in 68.4% of branches) or because the magnitude of fast rates in both traits were not correlated (in 9.5% of branches). There was no variation in either trait for the remaining 22.1% of branches.

chain Monte Carlo (MCMC), $P_{\text{MCMC}} = 9\%$) (Fig. 3a, consistent with Fig. 1f; Supplementary Table 9). This also suggests that evolution was decoupled in those branches—probably because of distinct selection pressures that acted separately on BMR and T_b . On the other hand, both traits evolved at a constant rate in 63.8% of branches for birds (Fig. 3c, consistent with Fig. 1a). In 32% of branches, only one trait evolved at fast rates while the other trait diverged at a constant rate (Fig. 3c, consistent with Fig. 1d, e). In the remaining 4.2% of branches, both traits evolved at faster rates, but the magnitudes of r were not statistically correlated ($P_{\text{MCMC}} = 16.9\%$) (Fig. 3c, consistent with Fig. 1f; Supplementary Table 10).

As rapid bursts in the evolution of BMR were not coupled with the evolutionary changes in T_b , we evaluated the alternative hypothesis that postulates that BMR evolved in response to T_a . This hypothesis suggests that colder environments increase the rate of heat loss from organisms and that this loss is subsequently compensated for by increases in BMR^{9–12}. These increases in BMR could have occurred over long periods of time because of global cooling¹⁸—generating a long-term

directional trend in BMR during the radiation of mammals and birds. This expectation is consistent with the plesiomorphic–apomorphic endothermy model^{6–8}. By assuming that BMR and T_b are coupled in endotherms and that they can both be used as a proxy for the degree of endothermy, the plesiomorphic–apomorphic endothermy model predicts a general tendency towards higher endothermic levels over time (from basoendothermic ancestors; Methods) associated with the global cooling during the Cenozoic era. However, global cooling is not the only source of variation in T_a . Long-term directional increases in BMR may have also been driven by historical dispersals of endotherms towards higher latitudes¹⁹. In either case, if a long-term decrease in T_a drove adaptation through increases in BMR, and T_b followed the same trajectory (as assumed by the plesiomorphic–apomorphic endothermy model), we expect to find a positive correlation between the branch-wise rates of BMR and the branch-wise rates of T_a . With this in mind, we also expect a positive trend towards higher values of BMR and T_b for basoendothermic ancestors and a negative trend towards lower T_a for warmer ancestral environments. We used the phylogenetic variable-rate regression model to estimate the branch-wise rates for T_a while accounting for latitude as, generally, T_a decreases from the equator to the poles (Methods and Supplementary Table 11).

The phylogenetic variable-rate regression model significantly improved the fit to the T_a data over the constant-rate regression model in both mammals and birds (Supplementary Table 11). T_a evolved at a constant rate in 21.2% of mammalian branches, and with rate heterogeneity in the remaining 78.8%—including 72.2% of branches with faster rates and 6.6% with slower rates ($r < 1$) (Fig. 2c). This indicates that most ancestral mammalian lineages (72.2%) faced abrupt historical changes in their T_a environment, while far fewer lineages (6.6%, most of which were bats) survived and continued to exist in similar thermal environments. In birds, 77.6% of branches show faster rates of change in T_a , 22.1% show changes at a constant rate and in only a single branch did the T_a change at a slower rate (Fig. 2f).

When branch-wise rates of mammalian BMR and T_a evolution were compared, we found that they were coupled in 74.9% of branches ($P_{\text{MCMC}} = 0\%$) (Fig. 3b, consistent with Fig. 1b; Supplementary Table 12). To evaluate further whether decreases in T_a were linked to increases in BMR in the 74.9% of mammals for which both traits were coupled (that is, to ascertain the direction of change), we evaluated the expected positive trend in BMR as a response to the long-term decrease in T_a . We conducted Bayesian phylogenetic regressions between extant values of these two variables (in turn) and the path-wise rates¹⁵ (sum of rate-scaled branches along the path from the root of the tree to each terminal species; Methods). We found a negative effect of path-wise rates on T_a across all mammals (Fig. 4b and Supplementary Table 14), which supports a long-term directional trend towards habitats with lower T_a over time. However, we did not find evidence for any trend in mammalian BMR evolution—increases and decreases in BMR showed equal probabilities in our sample (Supplementary Table 14). Our results suggest that in colder environments, in which resources were available to fuel metabolic elevation, selection favoured higher mammalian BMR²⁰. Another possibility might be that the increase in BMR was a correlated response to direct selection on other physiological traits, such as the maximum metabolic capacities for thermogenesis, for which the benefits outweigh the energetic cost of BMR elevation²⁰. Otherwise, selection may have always favoured decreases in BMR in an ever-colder environment²⁰.

In contrast to mammals, most avian branches that experienced rapid shifts in T_a did not show evidence for coupled changes in BMR—68.4% of branches had fast rates of T_a evolution but a constant rate of BMR evolution (Fig. 3d, consistent with Fig. 1d, e). Moreover, the small fraction of branches for which BMR evolved at fast rates (9.5%) were not linked to rapid shifts in T_a (Fig. 3d, consistent with Fig. 1f; Supplementary Table 13). Avian BMR did not show a positive evolutionary trend despite the fact that birds also experienced colder environments over time (Fig. 4d and Supplementary Table 15). Birds might not have responded to colder temperatures by changes in their BMR

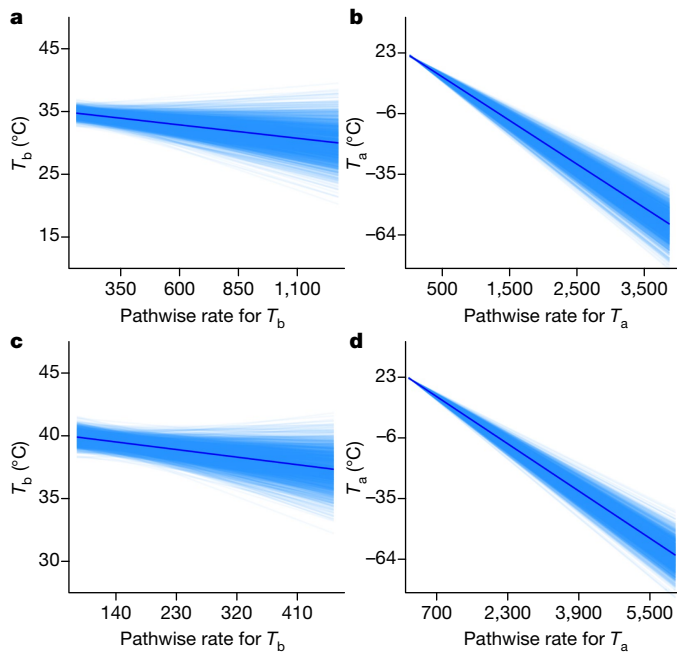


Fig. 4 | Mammals and birds evolved towards both colder T_b and T_a over their evolutionary history. a–d, Path-wise rates had a significant negative effect on mammalian T_b (a; $P_{\text{MCMC}} = 4\%$; $n = 502$ species) and avian T_b (c; $P_{\text{MCMC}} = 3\%$; $n = 367$ species) and on mammalian T_a (b; $P_{\text{MCMC}} = 0$; $n = 2,922$) and avian T_a (d; $P_{\text{MCMC}} = 0$; $n = 6,142$ species), supporting a negative macroevolutionary trend¹⁵ for both T_b and T_a in mammals and birds. Lighter blue and dark blue lines indicate the posterior distribution of slopes and the mean slope, respectively, estimated from the Bayesian phylogenetic generalized least squares (Methods).

because their lower thermal conductance may have helped them to retain internal heat⁹. Alternatively, other physiological strategies, such as torpor, may have been selected for in colder environments²¹.

Finally, we found a negative effect of path-wise rates on T_b in both mammals (Fig. 4a and Supplementary Table 14) and birds (Fig. 4c and Supplementary Table 15). This suggests that—on average—endotherms evolved towards colder bodies from warmer-bodied ancestors. These directional models predict a mean T_b of 35.3°C and 40.4°C for the most recent common ancestor (MRCA) of mammals and birds, respectively (Fig. 4a, c), suggesting that early birds and mammals were mesoendotherms rather than basoendotherms (Methods). This result does not support the idea that ancestral mammals could not attain $T_b > 30^\circ\text{C}$ owing to the increased metabolic rates that would be necessary to compensate for heat loss in cold environments²². However, if the $T_b - T_a$ differential (ΔT) determines how hot early mammals were, we expect that a mammalian MRCA with a T_b of 35.3°C could survive in an environment that was warm enough to have a low ΔT . Our model that describes the negative trend in T_a predicts that the MRCA of mammals lived in an environment that was 23°C on average (Fig. 4b), resulting in a ΔT of 15.3°C. This ancestral ΔT is very conservative compared with the ΔT values that have been observed in extant mammals. For example, there are small mammals that achieve a T_b higher than 39°C (such as *Microdipodops pallidus*¹⁶) and that can survive in environments of 11°C¹⁹ ($\Delta T = 28^\circ\text{C}$). Furthermore, some larger mammals have a stable T_b even in extreme environmental conditions—the Arctic hare (*Lepus arcticus*) can maintain its T_b of 38°C¹⁶ in temperatures as low as -12°C ¹⁹ ($\Delta T = 50^\circ\text{C}$).

Taken together, our results show that BMR was not coupled to T_b across the evolution of endothermic species. As environments became colder mammals survived by changing their BMR, while birds probably

survived owing to their high thermal insulation. Evaluating the isolated and/or combined effects of environmental variables on physiological attributes has implications for evidence-based projections for the future²³. In this sense, the previously unappreciated complexity, interplay and decoupled nature of the evolutionary history of BMR, T_b and T_a may point to the undetected resilience of endotherms in the face of modern global challenges.

Online content

Any methods, additional references, Nature Research reporting summaries, source data, extended data, supplementary information, acknowledgements, peer review information; details of author contributions and competing interests; and statements of data and code availability are available at <https://doi.org/10.1038/s41586-019-1476-9>.

Received: 5 November 2018; Accepted: 12 July 2019;

Published online 15 August 2019.

- Clarke, A. *Principles of Thermal Ecology. Temperature, Energy and Life* (Oxford Univ. Press, 2017)
- Gillooly, J. F., Brown, J. H., West, G. B., Savage, V. M. & Charnov, E. L. Effects of size and temperature on metabolic rate. *Science* **293**, 2248–2251 (2001).
- Clarke, A. & Pörtner, H.-O. Temperature, metabolic power and the evolution of endothermy. *Biol. Rev. Camb. Philos. Soc.* **85**, 703–727 (2010).
- Kemp, T. S. The origin of mammalian endothermy: a paradigm for the evolution of complex biological structure. *Zool. J. Linn. Soc.* **147**, 473–488 (2006).
- Brown, J. H., Gillooly, J. F., Allen, A. P., Savage, V. M. & West, G. B. Towards a metabolic theory of ecology. *Ecology* **85**, 1771–1789 (2004).
- Lovegrove, B. G. The evolution of endothermy in Cenozoic mammals: a plesiomorphic–apomorphic continuum. *Biol. Rev. Camb. Philos. Soc.* **87**, 128–162 (2012).
- Lovegrove, B. G. The evolution of mammalian body temperature: the Cenozoic supraendothermic pulses. *J. Comp. Physiol. B* **182**, 579–589 (2012).
- Lovegrove, B. G. A phenology of the evolution of endothermy in birds and mammals. *Biol. Rev. Camb. Philos. Soc.* **92**, 1213–1240 (2017).
- Fristoe, T. S. et al. Metabolic heat production and thermal conductance are mass-independent adaptations to thermal environment in birds and mammals. *Proc. Natl Acad. Sci. USA* **112**, 15934–15939 (2015).
- Naya, D. E., Naya, H. & White, C. R. On the interplay among ambient temperature, basal metabolic rate, and body mass. *Am. Nat.* **192**, 518–524 (2018).
- White, C. R., Blackburn, T. M., Martin, G. R. & Butler, P. J. Basal metabolic rate of birds is associated with habitat temperature and precipitation, not primary productivity. *Proc. R. Soc. Lond. B* **274**, 287–293 (2007).
- Jetz, W., Freckleton, R. P. & McKechnie, A. E. Environment, migratory tendency, phylogeny and basal metabolic rate in birds. *PLoS ONE* **3**, e3261 (2008).
- Venditti, C., Meade, A. & Pagel, M. Multiple routes to mammalian diversity. *Nature* **479**, 393–396 (2011).
- Rabosky, D. L. Automatic detection of key innovations, rate shifts, and diversity-dependence on phylogenetic trees. *PLoS ONE* **9**, e89543 (2014).
- Baker, J., Meade, A., Pagel, M. & Venditti, C. Adaptive evolution toward larger size in mammals. *Proc. Natl Acad. Sci. USA* **112**, 5093–5098 (2015).
- Clarke, A., Rothery, P. & Isaac, N. J. B. Scaling of basal metabolic rate with body mass and temperature in mammals. *J. Anim. Ecol.* **79**, 610–619 (2010).
- Baker, J., Meade, A., Pagel, M. & Venditti, C. Positive phenotypic selection inferred from phylogenies. *Zool. J. Linn. Soc.* **118**, 95–115 (2016).
- Zachos, J., Pagani, M., Sloan, L., Thomas, E. & Billups, K. Trends, rhythms, and aberrations in global climate 65 Ma to present. *Science* **292**, 686–693 (2001).
- Rolland, J. et al. The impact of endothermy on the climatic niche evolution and the distribution of vertebrate diversity. *Nat. Ecol. Evol.* **2**, 459–464 (2018).
- Swanson, D. L., McKechnie, A. E. & Vézina, F. How low can you go? An adaptive energetic framework for interpreting basal metabolic rate variation in endotherms. *J. Comp. Physiol. B* **187**, 1039–1056 (2017).
- Körtner, G., Brigham, R. M. & Geiser, F. Winter torpor in a large bird. *Nature* **407**, 318 (2000).
- Crompton, A. W., Taylor, C. R. & Jagger, J. A. Evolution of homeothermy in mammals. *Nature* **272**, 333–336 (1978).
- Bozinovic, F. & Pörtner, H.-O. Physiological ecology meets climate change. *Ecol. Evol.* **5**, 1025–1030 (2015).
- Lieberman, B. S. & Dudgeon, S. An evaluation of stabilizing selection as a mechanism for stasis. *Palaeogeogr. Palaeoclimatol. Palaeoecol.* **127**, 229–238 (1996).

Publisher's note: Springer Nature remains neutral with regard to jurisdictional claims in published maps and institutional affiliations.

© The Author(s), under exclusive licence to Springer Nature Limited 2019

METHODS

Data. We used a time-calibrated phylogenetic tree of extant mammals ($n = 3,321$)²⁵, and data for M , BMR and T_b were obtained from a previously published study¹⁶ ($n = 632$). After identifying species in the tree that have trait information, we obtained a final mammalian dataset of 502 species, which includes representatives from 15 orders (Supplementary Information).

For birds, we used the consensus time-calibrated tree from a previous study¹⁹. This tree was inferred from the samples of trees that have previously been published²⁶. Data for BMR, T_b and M were obtained from a previously published study⁹. After matching this database with the phylogenetic tree, we obtained a final sample of 164 species, which includes representatives from 21 orders (Supplementary Information). The dataset used to evaluate evolutionary trends in T_b (see below) has previously been published²⁷, and contains 367 species with phylogenetic information.

Data for T_a and latitude for extant mammals and birds were extracted from a previous publication¹⁹. These datasets include 2,922 species of mammals and 6,142 species of birds, which have phylogenetic information. The T_a for extant endothermic species is the temperature of the environments that birds and mammals inhabit today—measured as the mean ambient temperature for the mid-point latitude of each species distribution¹⁹. The T_a at which a species exists today may not be a heritable trait per se. However, the evolution of T_a can still be inferred using phylogenetic methods as habitat selection reflects adaptations of the species (traits) to some characteristics of the environment. This interrelationship should leave a phylogenetic signal in the T_a at which endothermic species live. Accordingly, we found a significant phylogenetic signal in the T_a of both mammals ($\lambda_{\text{PosteriorMean}} = 0.77$; Bayes factor = 665) and birds ($\lambda_{\text{PosteriorMean}} = 0.8$; Bayes factor = 1,404). Furthermore, the phylogenetic signal for T_a is very high ($\lambda = 1$) in birds and mammals when estimated using the median- r scaled tree.

Finally, to evaluate the endothermic levels for the MRCA of mammals and birds that have previously been proposed^{7,8}, we followed this categorization of endothermic species: as basoendotherms ($T_b^{\text{Birds}} < 40.4^\circ\text{C}$; $T_b^{\text{Mammals}} < 35.0^\circ\text{C}$), mesoendotherma ($40.4^\circ\text{C} \leq T_b^{\text{Birds}} \leq 42.5^\circ\text{C}$; $35^\circ\text{C} \leq T_b^{\text{Mammals}} \leq 37.9^\circ\text{C}$) and supraendotherms ($T_b^{\text{Birds}} > 42.5^\circ\text{C}$; $T_b^{\text{Mammals}} > 37.9^\circ\text{C}$).

Inferring the branch-wise rates of evolution. We identified heterogeneity in the rate of evolution along phylogenetic branches (branch-wise rates) by dividing the rate into two parameters: a background rate parameter (σ_b^2), which assumes that changes in the trait of interest (for example, BMR) are drawn from an underlying Brownian process, and a second parameter, r , which identifies a branch-specific rate shift. A full set of branch-wise rates are estimated by adjusting the lengths of each branch in a time-calibrated tree (stretching or compressing a branch is equivalent to increasing or decreasing the phenotypic rate of change relative to the underlying Brownian rate of evolution). Branch-wise rates are defined by a set of branch-specific scalars r ($0 < r < \infty$) that scale each branch to optimize the phenotypic rate of change to a Brownian process ($\sigma_b^2 \times r$). If phenotypic change occurred at accelerated (faster) rates along a specific branch of the tree, then $r > 1$ and the branch is stretched. Decelerated (slower) rates of evolution are detected by $r < 1$ and the branch is compressed. If the trait evolves at a constant rate along a branch, then the branch will not be modified (that is, $r = 1$).

We estimated the r values of evolution for BMR, T_b , and T_a using the phylogenetic variable-rate regression model in a Bayesian framework¹⁷. This model is designed to automatically detect shifts in the rate of trait evolution across phylogenetic branches while accounting for a relationship with another trait or traits across values for extant species. This approach enables the simultaneous estimation of both an overall relationship between—for instance—BMR as a function of M and T_b across extant species, and any shifts in the rate r that apply to the phylogenetically structured residual variance in the relationship. As residual variance is explained by shifts in rate across phylogenetic branches (r) we can, for example, determine how much BMR has changed in the past after accounting for its covariation with M and T_b in the present (the relationship between the values across extant species). Thus, if the amounts of change in BMR along individual phylogenetic branches were coupled with the amounts of change of T_b , then we should find the r_{BMR} values to be positively associated with the r_{T_b} values. The branch-wise rates for T_b evolution can be estimated while accounting for its covariation with other traits or factor across extant species. Previous studies on the association between BMR and T_b that only used values for extant species have not evaluated the association in evolutionary terms, even when they use phylogenetic methods.

We evaluated 24 phylogenetic variable-rate regression models and 24 phylogenetic constant-rate regression models (Supplementary Tables 1–8). The selection of the regression model was conducted using Bayes factors (B) using marginal likelihoods estimated by stepping stone sampling. B is calculated as the double of the difference between the log marginal likelihood of the complex model and the simple model. By convention, $B > 2$ indicates positive evidence for the complex model, $B = 5$ –10 indicates strong support and $B > 10$ is considered very strong

support²⁸. We inferred the r_{BMR} and r_{T_b} values with the phylogenetic variable-rate regression models that best fit the data for our samples of mammals and birds (Supplementary Tables 7, 8). We also estimated the r_{T_a} values after accounting for the effect of the latitude of the distribution of species (Supplementary Table 11) and, consequently, we accounted for the geographical variation of T_a across the distribution of extant species. We used BayesTraits v.3.0²⁹ to detect the magnitude and location of r in a Bayesian MCMC reversible-jump framework, which generates a posterior distribution of trees with scaled branches lengths according to the rate of evolution. There is no limit or prior expectation in the number of the r branch scalars, r numbers vary from zero (no branch is scaled) to n , in which n is the number of branches in the phylogenetic tree. Regarding the values of each r parameter, we used a gamma prior, with $\alpha = 1.1$ and a β parameter that is rescaled such that the median of the distribution is equal to 1. With this setting, the numbers of the rate increases and decreases that are proposed are balanced¹³. We ran 50,000,000 iterations sampling every 25,000 to ensure chain convergence and independence in model parameters in BMR and T_b analyses. We discarded the first 25,000 iterations as burn-in. For the T_a analysis in mammals, we ran 200,000,000 iterations sampling every 100,000, and we discarded the first 100,000 iterations as burn-in. For T_a analysis in birds, we ran 400,000,000 iterations discarding the first 100,000,000 as burn-in, and we sampled every 200,000. Regression coefficients were judged to be significant according to a calculated P_{MCMC} value for each posterior of regression coefficients for cases in which $< 5\%$ of samples in the posterior distribution crossed zero; this indicates that the coefficient is significantly different from zero.

Testing the relationship between the branch-wise rates of evolution. We first estimated the consensus branch-scaled tree for BMR and T_b from the posterior sample of branch-scaled trees obtained with the phylogenetic variable-rate regression model. The consensus branch-scaled tree was generated by using the median r from the posterior distribution. We evaluated the correlation between the r_{BMR} and r_{T_b} values using a Bayesian generalized least squares regression in BayesTraits v.3.0. The same analyses were conducted to evaluate the correlation between r_{BMR} and r_{T_a} . We used a uniform prior for the β (slope coefficient), which ranged from -100 to 100 . We ran 50,000,000 iterations sampling every 25,000 to ensure chain convergence and independence in model parameters. We discarded the first 25,000 iterations as burn-in. Significance of regression coefficients was determined as above.

Detecting trends. We evaluated the direction of change in BMR, T_b and T_a across all mammals and birds using the path-wise rates of these variables (Supplementary Tables 15, 16). The path-wise rate is the sum of all of the rate-scaled branches along the path of a species, which lead from the root (the MRCA) to the tips of the tree, and it accounts for the total amount of change that the species has experienced during its evolution¹⁵. If high path-wise rates have disproportionately been associated with trait increases or decreases, we expect to find that species with greater path-wise rates will have high or low trait values in the present. For instance, if ancestral mammals experienced progressively colder environmental temperatures owing to climate change or colonization of colder habitats as they were evolving from their MRCA, we expect a negative correlation between the path-wise rate of T_a and the T_a of extant species. We performed six Bayesian PGLS regressions in BayesTraits v.3.0 to evaluate the relationship between BMR, T_b , T_a and their path-wise rates (Supplementary Tables 15, 16). We used a uniform prior for the β (slope coefficients) that ranged from -100 to 100 to allow all possible values to have an equal probability. Finally, we ran 50,000,000 iterations sampling every 25,000 to ensure chain convergence and independence in model parameters. We discarded the first 25,000 iterations as burn-in. Significance of regression slopes was determined as above.

Reporting summary. Further information on research design is available in the Nature Research Reporting Summary linked to this paper.

Data availability

No new data were generated for this study. The data used for this paper are available from the original sources cited in the Methods and Supplementary Information.

- Fritz, S. A., Bininda-Emonds, O. R. & Purvis, A. Geographical variation in predictors of mammalian extinction risk: big is bad, but only in the tropics. *Ecol. Lett.* **12**, 538–549 (2009).
- Jetz, W., Thomas, G. H., Joy, J. B., Hartmann, K. & Mooers, A. O. The global diversity of birds in space and time. *Nature* **491**, 444–448 (2012).
- Clarke, A. & Rothery, P. Scaling of body temperature in mammals and birds. *Funct. Ecol.* **22**, 58–67 (2008).
- Raftery, A. E. in *Markov Chain Monte Carlo in Practice* (eds Gilks, W. R. et al.) 163–187 (Chapman & Hall, 1996).
- Pagel, M., Meade, A. & Barker, D. Bayesian estimation of ancestral character states on phylogenies. *Syst. Biol.* **53**, 673–684 (2004).

Acknowledgements We thank C. O'Donovan, J. Baker, M. Sakamoto and A. N. Campoy for helpful discussion of the manuscript. A. Clarke supplied data for

mammals and birds. This work is part of the PhD thesis of J.A.-L., supported by the CONICYT Doctoral Fellowship 21130943. C.V. was supported by the Leverhulme Trust (RPG-2013-185 and RPG-2017-071). C.E.H. and E.R.-S. were supported by FONDECYT grants 1170815 and 1170486.

Author contributions J.A.-L., C.E.H., E.R.-S. and C.V. contributed to all aspects of this work.

Competing interests The authors declare no competing interests.

Additional information

Supplementary information is available for this paper at <https://doi.org/10.1038/s41586-019-1476-9>.

Correspondence and requests for materials should be addressed to J.A. or C.V.
Peer review information *Nature* thanks Olaf Bininda-Emonds, Isabella Capellini and the other, anonymous, reviewer(s) for their contribution to the peer review of this work.

Reprints and permissions information is available at <http://www.nature.com/reprints>.

Reporting Summary

Nature Research wishes to improve the reproducibility of the work that we publish. This form provides structure for consistency and transparency in reporting. For further information on Nature Research policies, see [Authors & Referees](#) and the [Editorial Policy Checklist](#).

Statistical parameters

When statistical analyses are reported, confirm that the following items are present in the relevant location (e.g. figure legend, table legend, main text, or Methods section).

n/a Confirmed

- | | | |
|-------------------------------------|-------------------------------------|---|
| <input type="checkbox"/> | <input checked="" type="checkbox"/> | The <u>exact sample size</u> (n) for each experimental group/condition, given as a discrete number and unit of measurement |
| <input checked="" type="checkbox"/> | <input type="checkbox"/> | An indication of whether measurements were taken from distinct samples or whether the same sample was measured repeatedly |
| <input type="checkbox"/> | <input checked="" type="checkbox"/> | The statistical test(s) used AND whether they are one- or two-sided
<i>Only common tests should be described solely by name; describe more complex techniques in the Methods section.</i> |
| <input type="checkbox"/> | <input checked="" type="checkbox"/> | A description of all covariates tested |
| <input checked="" type="checkbox"/> | <input type="checkbox"/> | A description of any assumptions or corrections, such as tests of normality and adjustment for multiple comparisons |
| <input type="checkbox"/> | <input checked="" type="checkbox"/> | A full description of the statistics including <u>central tendency</u> (e.g. means) or other basic estimates (e.g. regression coefficient) AND <u>variation</u> (e.g. standard deviation) or associated <u>estimates of uncertainty</u> (e.g. confidence intervals) |
| <input checked="" type="checkbox"/> | <input type="checkbox"/> | For null hypothesis testing, the test statistic (e.g. F , t , r) with confidence intervals, effect sizes, degrees of freedom and P value noted
<i>Give P values as exact values whenever suitable.</i> |
| <input type="checkbox"/> | <input checked="" type="checkbox"/> | For Bayesian analysis, information on the choice of priors and Markov chain Monte Carlo settings |
| <input checked="" type="checkbox"/> | <input type="checkbox"/> | For hierarchical and complex designs, identification of the appropriate level for tests and full reporting of outcomes |
| <input checked="" type="checkbox"/> | <input type="checkbox"/> | Estimates of effect sizes (e.g. Cohen's d , Pearson's r), indicating how they were calculated |
| <input checked="" type="checkbox"/> | <input type="checkbox"/> | Clearly defined error bars
<i>State explicitly what error bars represent (e.g. SD, SE, CI)</i> |

Our web collection on [statistics for biologists](#) may be useful.

Software and code

Policy information about [availability of computer code](#)

Data collection

No software was used for data collection.

Data analysis

All analyses in this study were done using BayesTraits version 3 available at <http://www.evolution.rdg.ac.uk/BayesTraitsV3/BayesTraitsV3.html>

For manuscripts utilizing custom algorithms or software that are central to the research but not yet described in published literature, software must be made available to editors/reviewers upon request. We strongly encourage code deposition in a community repository (e.g. GitHub). See the Nature Research [guidelines for submitting code & software](#) for further information.

Data

Policy information about [availability of data](#)

All manuscripts must include a [data availability statement](#). This statement should provide the following information, where applicable:

- Accession codes, unique identifiers, or web links for publicly available datasets
- A list of figures that have associated raw data
- A description of any restrictions on data availability

The authors declare that data supporting the finding of this study is available in previous studies listed in the references.

Field-specific reporting

Please select the best fit for your research. If you are not sure, read the appropriate sections before making your selection.

Life sciences Behavioural & social sciences Ecological, evolutionary & environmental sciences

For a reference copy of the document with all sections, see [nature.com/authors/policies/ReportingSummary-flat.pdf](https://www.nature.com/authors/policies/ReportingSummary-flat.pdf)

Life sciences study design

All studies must disclose on these points even when the disclosure is negative.

Sample size	Sample size was determined by taxa present in the phylogeny which also had phenotypic, environmental, and geographic data. For mammals, 502 species had data for basal metabolic rate, body temperature, and body mass. 2922 species had data for ambient temperature and latitude. For birds, 164 species had data for basal metabolic rate, body temperature, and body mass. 6142 species had data for ambient temperature and latitude. The reversible-jump procedure we use in our analyses is specifically designed to identify significant shifts in the rate of evolution. Where statistical power is too low to detect a shift (e.g. n is low) no such shift will be identified.
Data exclusions	We excluded species that did not have data for all phenotypic variables or for ambient temperature and latitude.
Replication	Five replicates of rates of evolution inference, evolutionary trends, and correlation between rates, produced qualitatively the same results.
Randomization	This is not relevant to our study because it is not experimental in this way.
Blinding	Blinding is not relevant to our study as it is not experimental in this way.

Reporting for specific materials, systems and methods

Materials & experimental systems

n/a	Involvement in the study
<input checked="" type="checkbox"/>	<input type="checkbox"/> Unique biological materials
<input checked="" type="checkbox"/>	<input type="checkbox"/> Antibodies
<input checked="" type="checkbox"/>	<input type="checkbox"/> Eukaryotic cell lines
<input checked="" type="checkbox"/>	<input type="checkbox"/> Palaeontology
<input checked="" type="checkbox"/>	<input type="checkbox"/> Animals and other organisms
<input checked="" type="checkbox"/>	<input type="checkbox"/> Human research participants

Methods

n/a	Involvement in the study
<input checked="" type="checkbox"/>	<input type="checkbox"/> ChIP-seq
<input checked="" type="checkbox"/>	<input type="checkbox"/> Flow cytometry
<input checked="" type="checkbox"/>	<input type="checkbox"/> MRI-based neuroimaging